energies

MDPI

Article

Thermal Impact Analysis of Circulating Current in High Power Modular Online Uninterruptible Power Supplies Application

Chi Zhang, Josep M. Guerrero * and Juan C. Vasquez

Department of Energy Technology, Aalborg University, Pontoppidanstraede 111, 9220 Aalborg, Denmark; qantoo.zc@gmail.com (C.Z.); juq@et.aau.dk (J.C.V.)

* Correspondence: joz@et.aau.dk; Tel.: +45-20378262

Academic Editor: Chunhua Liu

Received: 17 October 2016; Accepted: 26 December 2016; Published: 4 January 2017

Abstract: In modular uninterruptible power supplies (UPSs), several DC/AC modules are required to work in parallel. This structure allows the system to be more reliable and flexible. These DC/AC modules share the same DC bus and AC critical bus. Module differences, such as filter inductor, filter capacitor, control parameters, and so on, will make it possible for the potential zero sequence current to flow among the modules. This undesired type of circulating current will bring extra losses to the power semiconductor devices in the system, which should be paid special attention in high power application scenarios. In this paper, plug'n'play modules and cycle control are discussed and validated through experimental results. Moreover, potential zero sequence circulating current impact on power semiconductor devices thermal performance is also analyzed in this paper.

Keywords: modular; online uninterruptible power supplies (UPSs) system; thermal evaluation

1. Introduction

Recently, more and more advanced technologies are entering human beings everyday life. A large number of modern electrical facilities, such as communication equipment, IT facilities, medical equipment, and so on, are widely used in both the industrial field and daily life [1]. As a result, the utility suffers great challenges in order to provide a clean, continuous, and reliable electrical energy. On the other hand, with the prosperity of the renewable energy sources, more and more factories and offices tend to use a local smart utility system [2]. However, renewable energy sources are unpredictable. This will have negative impacts on the power quality that they provide. Consequently, uninterruptible power supply (UPS) system is receiving more and more attention from both researchers and industrial application engineers [3].

Based on IEC 62040-3, UPS system is able to be divided into three categories, namely offline UPS system, line interactive UPS system, and online UPS system. Compared with the other two, online UPS system, also known as double conversion UPS system, mainly aims at high power application scenarios due to its outstanding capability in output voltage control and decoupling of the utility and the load [4,5]. In order to improve UPS performance, a series of enhanced different online UPS structure is proposed in [6–8]. Among them, the modular concept is drawing more and more attention due to its attractive flexibility and expansibility. Consequently, when the system is required to be maintained or has module failure, a modular online UPS system is still able to operate normally by replacing to stop the damaged module.

Normally a number of DC/AC modules operates in parallel and shares the same DC bus and AC bus (as shown in Figure 1a) in a typical modular online UPS system. Thus, possible paths for potential zero sequence circulating current exist (which is marked by red in Figure 1b). It still has negative

impacts on losses and thermal distribution of the power semiconductor devices. The unbalanced losses and thermal distribution performances, especially in high power modular scenarios, are required to be investigated further, which can be a guidance concerning heat problems in designing the modular online UPS systems. In order to avoid such kinds of circulating current, a number of approaches are proposed, namely isolation [9–11], high impedance [12,13], synchronized issues [14–17], and active issues [18–20]. Isolation and high impedance issues will add extra devices into the system, such as extra DC sources, transformers, or inter-phase reactors and these will increase the UPS system cost. As such, it is not a cost effective and volume effective issue. As a result, synchronization and active issues are considered hereby.

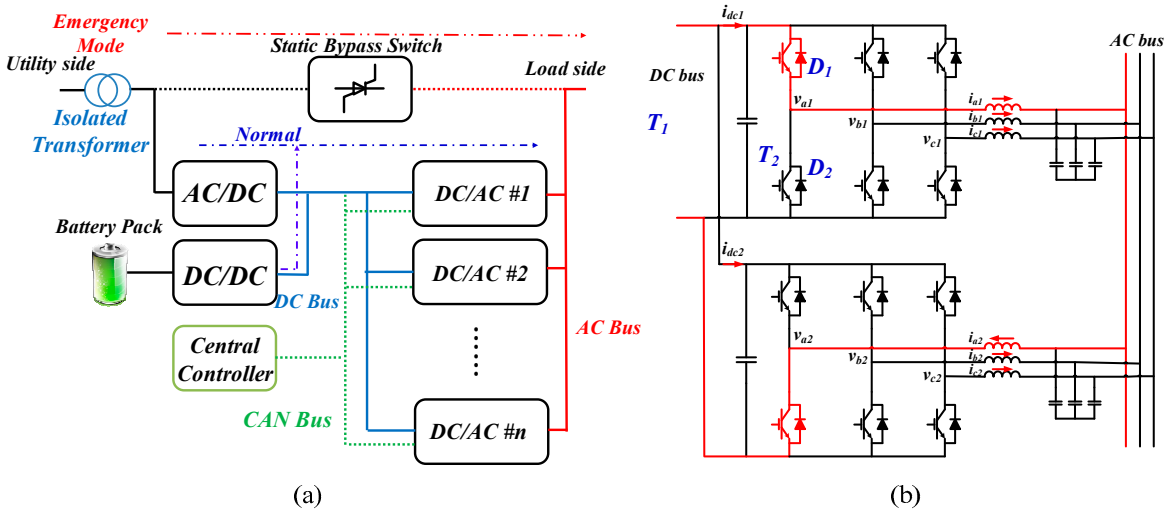

Figure 1. Modular uninterruptible power supplies (UPSs) system architecture and circulating current path: (**a**) modular UPS system structure; and (**b**) circulating current flowing path.

On the other hand, active power and reactive power of each of the DC/AC modules should be equally shared in order to minimize the active power circulating current. A number of parallel technologies have been proposed in [21–26], which can be categorized into two main types, namely communication based and communication-less. Since the mature digital signal processor (DSP) technology provides a smaller data transmit time delay, a communication based parallel technology is used here. By using virtual resistor and phase regulating methods, both active and reactive power are shared among all the modules.

In this paper, unsynchronized pulse width modulation (PWM) condition and physical parameters mismatch is considered since these two are more common in real applications. With the power devices thermal model proposed in [27], the thermal impedance of devices is edited in the simulation software PLECS. Thus, the temperature and losses of devices are able to be monitored to investigate the zero circulating current impacts on the losses and temperature of different power semiconductor devices.

This paper is organized as follows: Section 2 depicts the system control mechanism; Section 3 presents experimental results while the thermal analysis results are presented in Section 4; and Section 5 gives the final conclusion.

2. System Control Mechanism

As shown in Figure 1a, one three-phase AC/DC creates the DC bus for the DC/AC modules. Its control is considered in the conventional *dq* frame, which is descripted in [28] in detail. Several DC/AC modules are working in parallel and the detailed information for the modules is listed in Table 1.

Table 1. Module characteristics.

Nominal Power	Switch Frequency	DC Side	Bus Voltage	Bus Current
200 kW	5 kHz	700 V	230 V	290 A
Phase Number	**Topology**	**Filter**	**Inductor**	**Capacitance**
3	H_bridge	LC filter	1.8 mH	27 μF

2.1. Single Module Control

DC/AC modules inner loop uses conventional double control structure (voltage and current), which is considered in αβ frame:

$$G_v(s) = k_{pv} + \frac{k_{rv}s}{s^2 + {\omega_o}^2} + \sum_{h=5,7,11} \frac{k_{hrv}s}{s^2 + (\omega_o h)^2} \tag{1}$$

$$G_c(s) = k_{pc} + \frac{k_{rc}s}{s^2 + {\omega_o}^2} + \sum_{h=5,7,11} \frac{k_{hrc}s}{s^2 + (\omega_o h)^2} \tag{2}$$

with k_{pv}, k_{rv}, ω_o, k_{hrv}, h, k_{pc}, k_{rc}, and k_{hrc} being the voltage proportional term, fundamental frequency voltage resonant term, fundamental frequency, the hth harmonic voltage compensation term, harmonic order, current proportional term, fundamental frequency current resonant term, and the hth harmonic current compensation term, respectively. Two typical *PR*s are used due to its harmonic compensation capability.

2.2. Power Balance among Modules

As mentioned in [24], if the output impedance of the DC/AC modules is designated to be mainly resistive, the active power and reactive power that each DC/AC module injects into the AC bus are able to be regulated by voltage amplitude and phase, respectively, thus a virtual resistor and phase regulating loop are inserted into the control loop:

$$\delta_{nk} = \delta_{nkref} - k_{ph}Q_{nk} \tag{3}$$

$$v_{nk} = v_{nkref} - i_{Labc}Z_{vir} \tag{4}$$

Here n is the number of DC/AC module (1, 2, 3, ... , N), k is the phase order (a, b, c), V_{nkref} is the nominal voltage reference, Z_{vir} is the virtual resistor, δ_{nkref} is the nominal phase reference, k_{ph} is the phase regulating coefficients, and Q_{nk} is the reactive power of each phase of each DC/AC module.

2.3. Voltage Amplitude and Phase Synchronized

By measuring AC critical bus voltage, two typical Proportional Integrator (*PI*) controllers are used to keep online UPS output voltage tightly synchronized with the utility:

$$G_{v\_rec}(s) = k_{pv\_rec} + \frac{k_{iv\_rec}}{s} \tag{5}$$

$$G_{\delta\_rec}(s) = k_{p\delta\_rec} + \frac{k_{i\delta\_rec}}{s} \tag{6}$$

with k_{pv_rec}, k_{iv_rec}, $k_{p\delta\_rec}$, and $k_{i\delta\_rec}$ being voltage amplitude recovery proportional term, voltage amplitude recovery integral term, phase recover proportional term, and phase recover integral term, respectively. The overall control diagram is shown in Figure 2a.

2.4. Cycle and Plug'n'Play Control

The modular online UPS system is designed to be flexible, which means that any of the DC/AC modules can be plugged into or out of the system randomly due to module failure or maintenance reasons. Thus, some voltage overshoot or sag will occur in the AC critical bus, and this requires a control that can suppress the voltage overshoot or sag in a short transient time. In the standard IEC 62040-3, detailed requirements are included for the transient performance for an online UPS system, which is shown in Table 2.

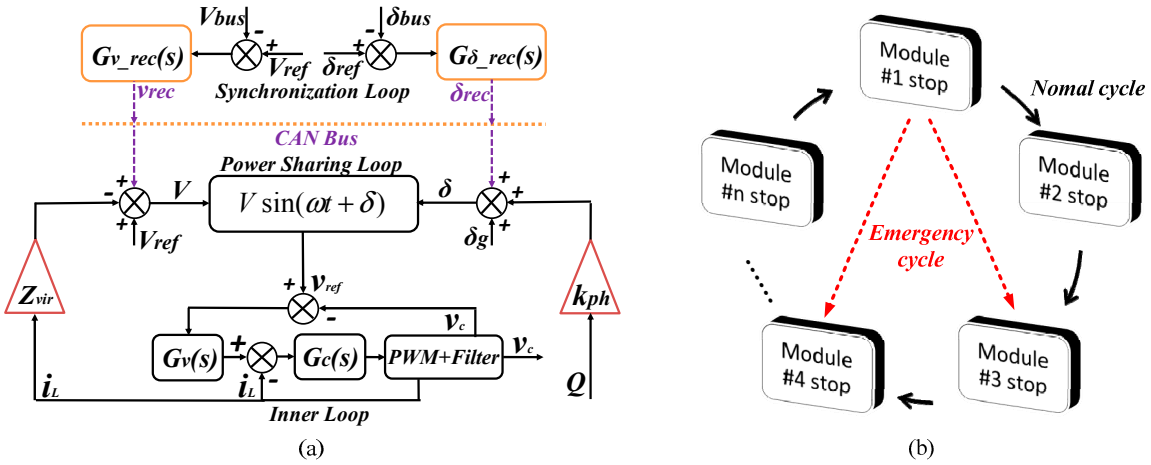

Figure 2. Control mechanism for modular UPS system: (**a**) overall control; and (**b**) plug'n'play control mechanism. PWM: pulse width modulation.

Table 2. Transient time requirements.

Load Type	Voltage Variation (%)	Dynamic Time Requirement (ms)
Linear Load	14	20–40
	12	40–60
	11	60–100
	10	100–1000
Nonlinear Load	12	40–60
	11	60–100
	10	100–1000

It can be seen that with a smaller voltage overshoot or sag, the transient time for the system can be a little longer. While designing the system, the overshoot or sag should be guaranteed that its amplitude should be controlled small as 10% compared with the nominal critical bus voltage amplitude. Thus, less stress will be put on the transient performance of the controller.

On the other hand, another reason for using modular UPS structure is that modules can operate in turns in order to allow all modules to be maintained or repaired equally, as shown in Figure 2b. When one of the modules disconnects with the AC critical bus, another module that has already finished the maintenance will start to connect with the AC critical bus at the same time in a fixed sequence, called Normal Cycle (NC). As a result, there is voltage transient during this process, which should be paid specific attention. Normally, such a cycle duration time is quite long in real applications, for instance, routinely numbering in the hours. However, in case of an emergency condition, such as module failures, the fixed sequence is interrupted and it will have a much shorter cycle duration time, which is called Emergency Cycle (EC).

Such kinds of plug'n'play modules will result in PWM unsynchronized problems, which will cause strong potential zero sequence circulating current. In addition, although each module is designated to

be the same, they still have many differences, such as filter inductors, capacitance, control parameters, and so on. These things will also provide the possibility for the zero sequence circulating current to occur.

3. Experimental Results

An experimental setup was built in the MicroGrid Intelligent Lab [28]. Four Danfoss converters were used. One of them works as AC/DC while the other three are working as the DC/AC modules. A control system was established in Matlab/Simulink and complied into the dSpace 1006 to achieve the real time control for the experimental setup.

3.1. Modules Plug'n'Play Performance

Hereby, one of the modules connected and disconnected with the AC critical bus in order to test the proposed control transient performance. Active and reactive power performance was monitored on the control desk in PC while the voltage real time performance was observed in scope.

At t_1, one module was plugging out of the system and both reactive and active power was well shared among the other two modules. At t_2, it plugged into the system again and the power was equally shared among the three modules, as shown in Figure 3a,b.

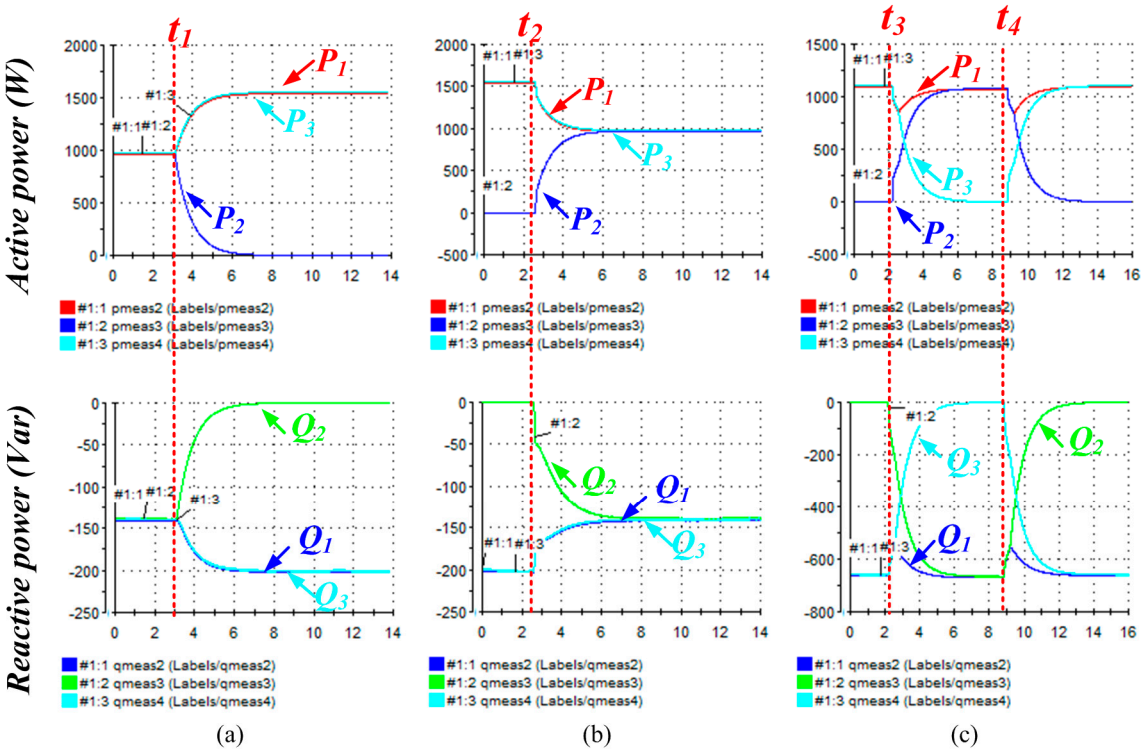

Figure 3. Power performance: (**a**) one module plug out; (**b**) module plug in; and (**c**) cycle control.

3.2. Cycle Control Transient Performance

The transient performance, when two DC/AC modules were switched, is presented in Figure 3c. In real applications, supervisory control monitors the operating condition of each of the DC/AC modules to decide operating rules. At t_3, module #3 was ordered to disconnect and rest for maintenance and module #2 was required to start working again in order to avoid overloading of the other modules, and at t_4, module #2 and #3 were switched for the second time. It can be observed that both active power and reactive power were well shared among the remaining modules.

The voltage detail at t_3 and t_4 is shown in Figure 4a,b. The voltage overshoot can be calculated through the scope, which is Δv = (620 − 570) V/570 V = 8.77% or (610 − 560) V/560 V = 8.92%. This value is below 10%, and the transient time is about three and a half utility periods (i.e., 70 ms), which is faster than 100 ms.

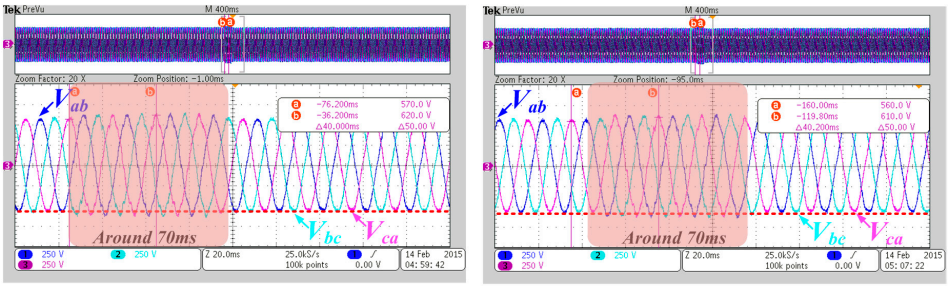

(a) (b)

Figure 4. Real time voltage waveform: (**a**) details at t_3; and (**b**) details at t_4.

4. Thermal Analysis Results

The thermal condition of power devices is an important issue that should be taken into consideration. It is tightly related with the cooling system of each DC/AC module, especially in high power application scenarios. Based on the thermal model shown in Figure 5, the thermal impedance from junction to case $Z_{(j\text{-}c)}$ is able to be treated as a four layer resistor-cpacitor (*RC*) network. For a specific power device, the information can be found in the manufacture datasheet. Since the thermal capacitance is mainly related with the dynamic process before steady state [29], big thermal capacitance of $Z_{T/D(c\text{-}h)}$ and $Z_{(h\text{-}a)}$ can be neglected in order to achieve a faster simulation.

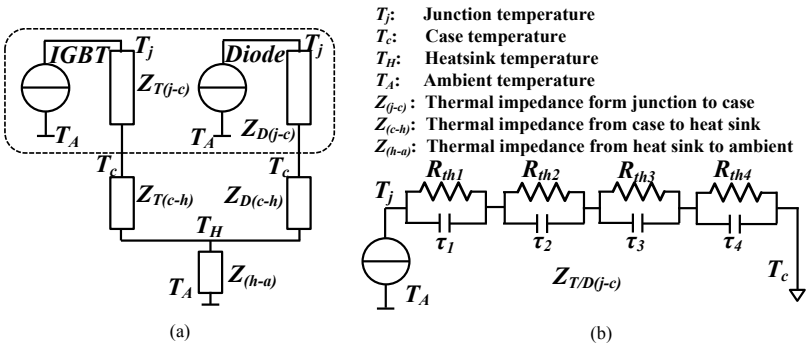

(a) (b)

Figure 5. Thermal model: (**a**) power devices thermal model; and (**b**) IGBT resistor-cpacitor (*RC*) network of $Z_{T/D(j\text{-}c)}$.

Based on the module information shown in Table 1, the IGBT pack 5SND-0800M170100 from ABB was chosen for the power semiconductor devices, whose thermal information is shown in Table 3 [30].

Table 3. Module thermal parameters.

Thermal Impedance	$Z_{T/D(j\text{-}c)}$			
	1	**2**	**3**	**4**
R_{iIGBT} (K/kW)	15.2	3.6	1.49	0.74
τ_{iIGBT} (ms)	202	20.3	2.01	0.52
R_{iDiode} (K/kW)	25.3	5.78	2.6	2.52
τ_{iIGBT} (ms)	210	29.6	7.01	1.49

With PLECS, the thermal impedance model of IGBT pack 5SND-0800M170100 can be edited in simulation. Thus, thermal information, including losses and temperature can be monitored. In [31], it mentions that normally DC/AC modules are designed to work in the load condition from 50% to 75%. As such, in the analysis, the load condition is considered from 50% to 100%, and losses and temperature information of T_1, T_2, D_1, and D_2 are discussed.

4.1. Single DC/AC Module

In order to compare with the modular UPS system, a single DC/AC module was simulated. Figure 6a,b presents the devices temperature and losses. It can be seen that the losses and temperature are distributed nearly balanced between T_1 and T_2, and D_1 and D_2.

Another critical parameter, namely the temperature fluctuation amplitude of the devices, is also important for power semiconductor devices. In Figure 6c,d, it can be observed that T_1 and T_2 share nearly the same temperature fluctuation amplitude, and a similar result can be seen for D_1 and D_2. Figure 6e shows the steady state temperature information in 100% load condition.

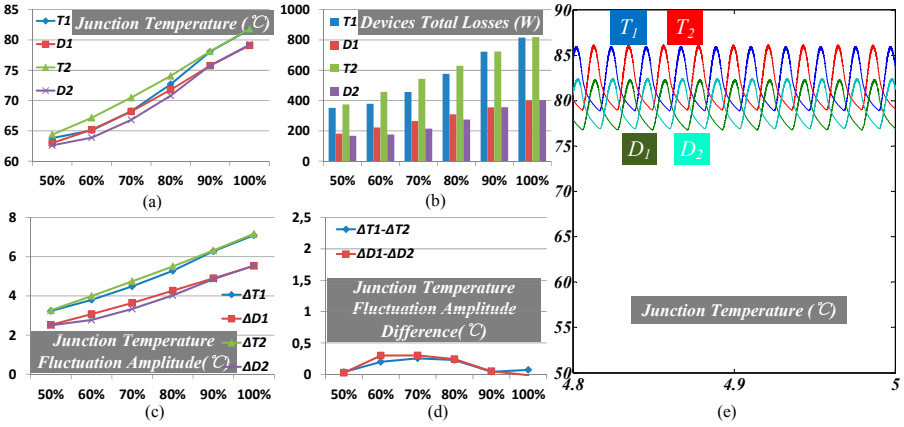

Figure 6. Single module result: (**a**) junction temperature; (**b**) devices loss; (**c**) junction temperature fluctuation; (**d**) temperature fluctuation difference; and (**e**) detailed temperature result in 100% load.

4.2. DC/AC Modules with Zero Sequence Circulating Current

In this condition, an unsynchronized PWM was given to the three DC/AC modules. Moreover, each module filter inductor was given a 30% difference to emulate the manufacturer difference. The control parameters were also different among different modules. Thus, an obvious circulating current can be observed, as shown in Figure 7a. It can be seen that there is some DC component; this is because both physical and control parameters differences will result in a small amount of active power circulating current.

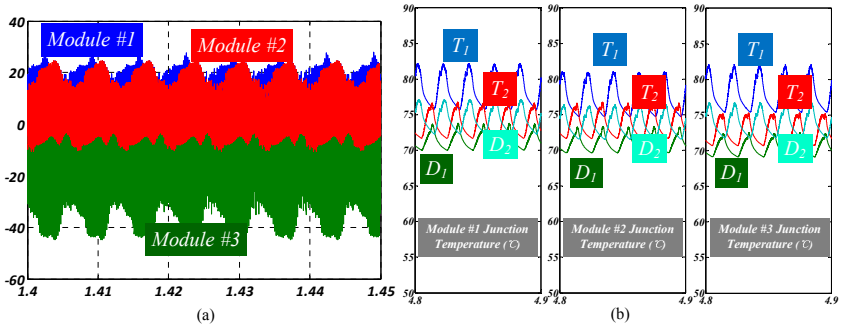

Figure 7. Circulating current and detailed temperature result with obvious circulating current: (**a**) three modules circulating current; and (**b**) detailed temperature in 100% load.

Figure 8a,b shows the losses and temperature information of each module. It can be seen that they are distributed unbalanced. In all the three modules, T_1 has a higher loss and temperature than T_2, and D_2 has a higher loss and temperature than D_1. A similar trend is also observed for the temperature fluctuation amplitude and fluctuation amplitude difference of the devices, as shown in Figure 8c. In Figure 7b, the steady state temperature for devices in 100% load condition is presented. It can be seen that the temperature is distributed in an unbalanced way. Since the thermal impedance of the heat sink is smaller in scale, the difference is not too obvious.

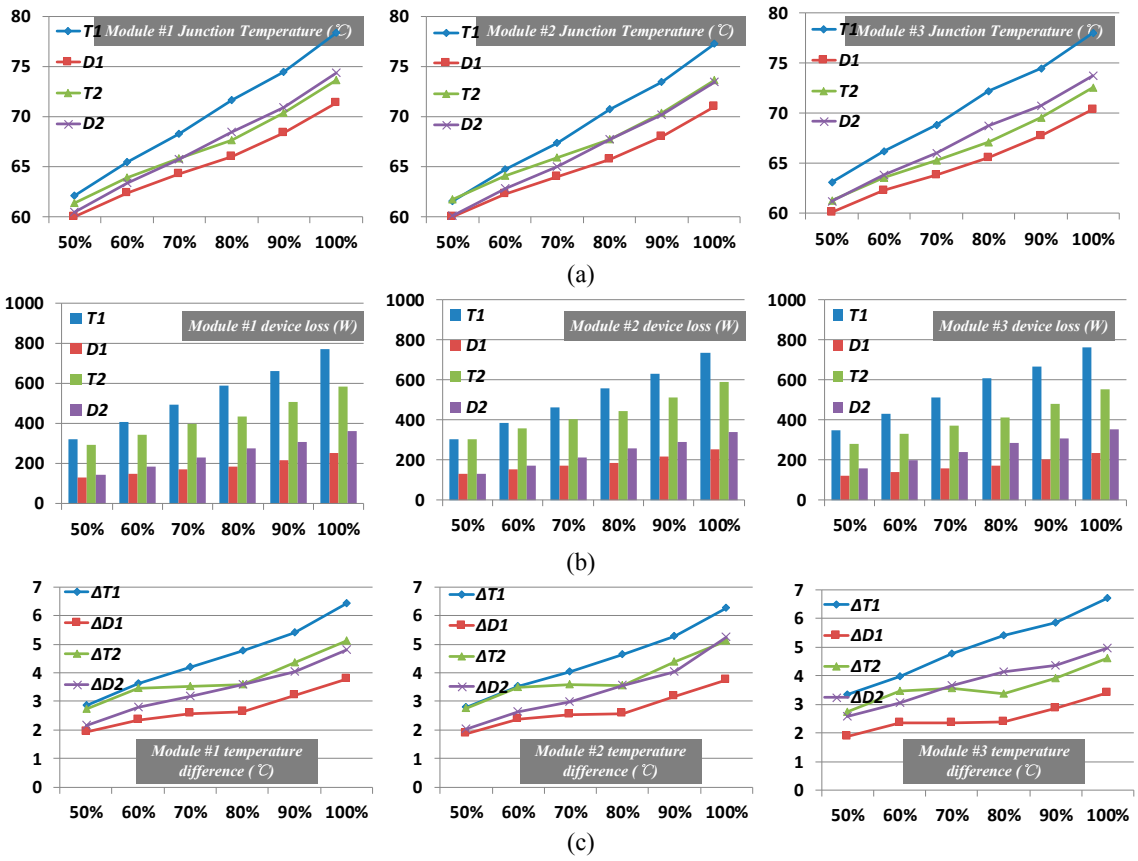

Figure 8. Thermal results of the modules with obvious circulating current flowing: (**a**) three module junction temperature; (**b**) devices losses; and (**c**) junction temperature differences.

4.3. DC/AC Modules with Suppressed Zero Sequence Circulating Current

Hereby, the zero sequence circulating current was suppressed. All the PWM for the three modules were synchronized, and zero vector operating time in the space vector modulation was tuned based on the active suppression method proposed in [18]. The zero sequence circulating current is presented in Figure 9a. It can be seen that the zero sequence circulating current was suppressed to a small amount of value. Figure 10a shows the losses of each module. All three modules shared the same loss distribution condition that T_2 has a higher loss and temperature than T_1, and D_1 had a higher loss and temperature than D_2. Consequently, they had the same temperature results, as shown in Figure 10b.

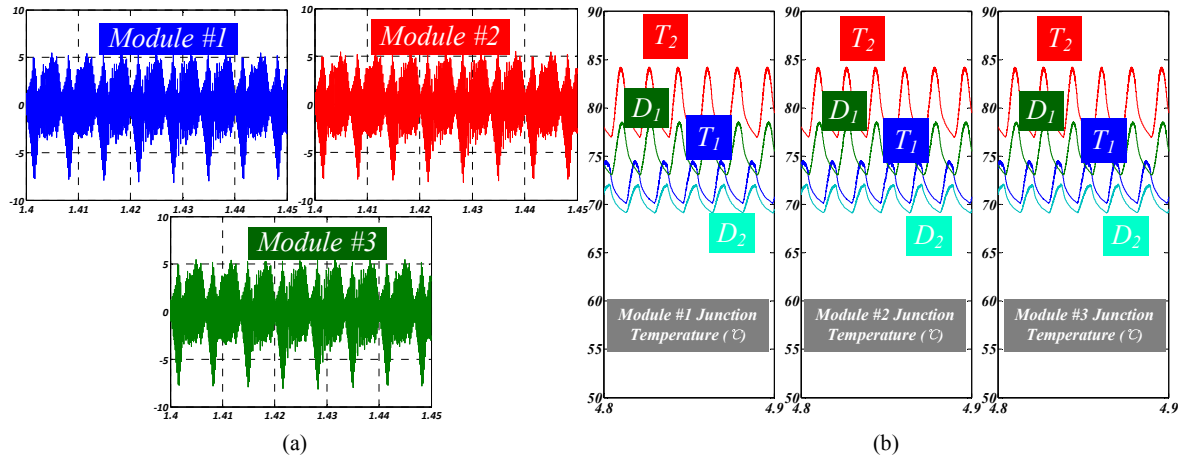

Figure 9. Circulating current and detailed temperature result without circulating current: (**a**) three modules circulating current; and (**b**) detailed temperature in 100% load.

As for the temperature fluctuation amplitude, three modules shared the same changing pattern. ΔT_2 first had a sudden increase at 90% load and then decreased. It was higher than ΔT_1. ΔD_1 decreased smoothly and was higher than ΔD_2. The fluctuation difference also presented a similar trend, as shown in Figure 10c.

The detailed temperature information of the three modules at 100% load condition is shown in Figure 9b. It can be seen that the T_2 had a higher loss and temperature than T_1, and D_1 had a higher loss and temperature than D_2.

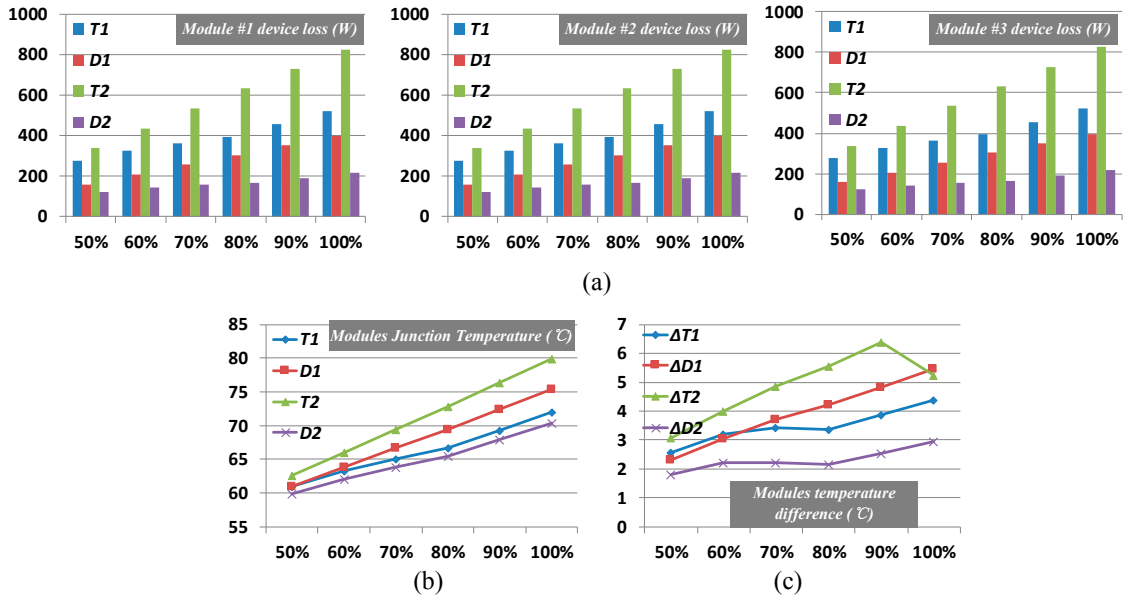

Figure 10. Thermal results of the modules without obvious circulating current flowing: (**a**) three module device losses; (**b**) junction temperature; and (**c**) junction temperature differences.

5. Conclusions

In this paper, the plug'n'play capability for a modular online UPS system was proposed and tested. Experimental results were provided to validate the proposed control steady and transient performance, which were able to meet the standard IEC 62040-3. Moreover, zero sequence circulating current impact on thermal and losses distribution of the power semiconductor devices was discussed.

Through simulation results, it can be concluded that while operating in different kinds of conditions associated with circulating current, T_1 had a higher temperature than T_2 while D_2 had a higher temperature than D_1. In order to suppress zero sequence circulating current, synchronization issues and zero vector time regulation were considered in this paper. However, such issues increased the temperature and losses of T_2, which was higher than T_1. Moreover, D_1 had a higher temperature than D_2.

Author Contributions: Chi Zhang developed the basic idea, simulation and wrote the paper. Juan C. Vasquez and Josep M. Guerrero helped to revise the paper.

Conflicts of Interest: The authors declare no conflicts of interest.

References

1. Majumder, R.; Ghosh, A.; Ledwich, G.; Zare, F. Load sharing and power quality enhanced operation of a distributed microgrid. *IET Renew. Power Gener.* **2009**, *3*, 109–119. [CrossRef]
2. Li, H.; Chen, Z. Overview of different wind generator systems and their comparisons. *IET Renew. Power Gener.* **2008**, *2*, 123–138. [CrossRef]
3. Chiang, H.C.; Ma, T.T.; Cheng, Y.H.; Chang, J.M.; Chang, W.N. Design and implementation of a hybrid regenerative power system combining grid-tie and uninterruptible power supply functions. *IET Renew. Power Gener.* **2010**, *4*, 85–99. [CrossRef]
4. Kim, E.-H.; Kwon, J.-M.; Kwon, B.-H. Transformerless three-phase on-line UPS with high performance. *IET Power Electron.* **2009**, *2*, 103–112. [CrossRef]
5. Yeh, C.C.; Manjrekar, M.D. A reconfigurable uninterruptible power supply system for multiple power quality applications. *IEEE Trans. Power Electron.* **2007**, *22*, 1361–1372. [CrossRef]
6. Zhao, B.; Song, Q.; Liu, W.; Xiao, Y. Next-generation multi-functional modular intelligent UPS system for smart grid. *IEEE Trans. Ind. Electron.* **2013**, *60*, 3602–3618. [CrossRef]
7. Shahparasti, M.; Yazdian, A.; Mohamadian, M.; Larijani, A.S.; Fatemi, A. Parallel uninterruptible power supplies based on Z-source inverters. *IET Power Electron.* **2012**, *5*, 1359–1366. [CrossRef]
8. Sato, E.K.; Kinoshita, M.; Yamamoto, Y.; Amboh, T. Redundant high-density high-efficiency double-conversion uninterruptible power system. *IEEE Trans. Ind. Appl.* **2010**, *46*, 1525–1533. [CrossRef]
9. Kawabata, T.; Higashino, S. Parallel operation of voltage source inverters. *IEEE Trans. Ind. Appl.* **1988**, *24*, 281–287. [CrossRef]
10. Dixon, J.W.; Ooi, B.T. Series and parallel operation of hysteresis current-controlled PWM rectifiers. *IEEE Trans. Ind. Appl.* **1989**, *25*, 644–651. [CrossRef]
11. Komatsuzaki, Y. Cross current control for parallel operating three phase inverter. In Proceedings of the 25th Annual IEEE Power Electronics Specialists Conference, Taipei, Taiwan, 20–25 June 1994; Volume 2, pp. 943–950.
12. Matsui, K.; Murai, Y.; Watanabe, M.; Kaneko, M.; Ueda, F. A pulse width-modulated inverter with parallel connected transistors using current-sharing reactors. *IEEE Trans. Power Electron.* **1993**, *8*, 186–191. [CrossRef]
13. Sato, Y.; Kataoka, T. Simplified control strategy to improve AC-input-current waveform of parallel-connected current-type PWM rectifiers. *IEE Proc. Electr. Power Appl.* **1995**, *142*, 246–254. [CrossRef]
14. Ogasawara, S.; Takagaki, J.; Akagi, H.; Nabae, A. A novel control scheme of a parallel current-controlled PWM inverter. *IEEE Trans. Ind. Appl.* **1992**, *28*, 1023–1030. [CrossRef]
15. Chunwei, S.; Rongxiang, Z.; Minglei, Z.; Zheng, Z. Operation method for parallel inverter system with common dc link. *IET Power Electron.* **2014**, *7*, 1138–1147.
16. Fukuda, S.; Matsushita, K. A control method for parallel-connected multiple inverter systems. In Proceedings of the 1998 Seventh International Conference on Power Electronics and Variable Speed Drives, London, UK, 21–23 September 1998; pp. 175–180.
17. Abe, R.; Nagai, Y.; Tsuyuki, K.; Nishikawa, H.; Shimamura, T.; Kawaguchi, A.; Shimada, K. Development of multiple space vector control for direct connected parallel current source power converters. In Proceedings of the Power Conversion Conference—Nagaoka 1997, Nagaoka, Japan, 3–6 August 1997; Volume 1, pp. 283–288.
18. Ye, Z.; Boroyevich, D.; Jae-Young, C.; Lee, F.C. Control of circulating current in two parallel three-phase boost rectifiers. *IEEE Trans. Power Electron.* **2002**, *17*, 609–615.

19. Jassim, B.M.H.; Zahawi, B.; Atkinson, D. Simple control method for parallel connected three-phase PWM converters. In Proceedings of the 6th IET International Conference on Power Electronics, Machines and Drives (PEMD 2012), Bristol, UK, 27–29 March 2012; pp. 1–5.
20. Shao, Z.; Zhang, X.; Wang, F.; Cao, R. Modeling and elimination of zero-sequence circulating currents in parallel three-level t-type grid-connected inverters. *IEEE Trans. Power Electron.* **2015**, *30*, 1050–1063. [CrossRef]
21. Wang, W.; Zeng, X.; Tang, X.; Tang, C. Analysis of microgrid inverter droop controller with virtual output impedance under non-linear load condition. *IET Power Electron.* **2014**, *7*, 1547–1556. [CrossRef]
22. Ma, H.; Lin, Z.; Lin, L.; Zhang, Y.; Wang, X. Flexible power weighting distribution for three-phase parallel inverters with networked control. *IET Power Electron.* **2015**, *8*, 1181–1194. [CrossRef]
23. Sun, X.; Tian, Y.; Chen, Z. Adaptive decoupled power control method for inverter connected DG. *IET Renew. Power Gener.* **2014**, *8*, 171–182. [CrossRef]
24. Guerrero, J.M.; Matas, J.; Vicuna, L.; Castilla, M.; Miret, J. Decentralized Control for Parallel Operation of Distributed Generation Inverters Using Resistive Output Impedance. *IEEE Trans. Ind. Electron.* **2007**, *54*, 994–1004. [CrossRef]
25. Planas, E.; Gil-de-Muro, A.; Andreu, J.; Kortabarria, I.; de Alegría, I.M. Design and implementation of a droop control in d-q frame for islanded microgrids. *IET Renew. Power Gener.* **2013**, *7*, 458–474. [CrossRef]
26. Nutkani, I.U.; Poh Chiang, L.; Blaabjerg, F. Cost-based droop scheme with lower generation costs for microgrids. *IET Power Electron.* **2014**, *7*, 1171–1180. [CrossRef]
27. *ABB Application Note: Applying IGBTs*; ABB Switzerland Ltd Semiconductors: Lenzburg, Switzerland, 2007.
28. Intelligent MicroGrids Laboratory. Available online: http://www.microgrids.et.aau.dk (accessed on 1 July 2016).
29. Wei, L.; McGuire, J.; Lukaszewski, R.A. Analysis of PWM frequency control to improve the lifetime of PWM inverter. In Proceedings of the 2009 IEEE Energy Conversion Congress and Exposition (ECCE 2009), San Jose, CA, USA, 20–24 September 2009; pp. 900–907.
30. *ABB Hipak, IGBT Module 5SND 0800M170100*; ABB Switzerland Ltd Semiconductors: Lenzburg, Switzerland, 2014.
31. *SG Series UPS 10–600 kVA Three Phase 400 Vac with Ultra-High Efficiency eBoost^{TM} Technology*; General Electric Company: Boston, MA, USA, 2013.

© 2017 by the authors; licensee MDPI, Basel, Switzerland. This article is an open access article distributed under the terms and conditions of the Creative Commons Attribution (CC-BY) license (http://creativecommons.org/licenses/by/4.0/).